

Magnetic Structure, Magnetization, and Short-Range Spin Correlations in the Ising Linear-Chain Antiferromagnet $\text{CsCoCl}_3 \cdot 2\text{H}_2\text{O}$

A. L. M. Bongaarts*

Department of Physics, Eindhoven University of Technology, Eindhoven, The Netherlands

and

B. van Laar

Reactor Centrum Nederland, Petten (Nh), The Netherlands

(Received 3 March 1972)

The magnetic space group and structure of $\text{CsCoCl}_3 \cdot 2\text{H}_2\text{O}$ have been confirmed. From the intensity of the Bragg scattering the magnetization-vs-temperature curve has been determined. It agrees closely with that obtained from NMR work and follows the power law $M(T)/M(0) = 2.34(1 - T/T_N)^{0.44}$ in the range $3.20 \leq T < T_N = 3.40$ K. Intrachain and interchain spin-correlation lengths have been determined. Between T_N and 4.2 K, the intrachain correlation remains practically constant while the interchain correlation steeply decreases with increasing temperature, thus giving rise to the formation of a linear-chain system. An estimate for the intrachain exchange leads to $25 < |J_a| < 35$ K.

I. INTRODUCTION

The crystal structure of $\text{CsCoCl}_3 \cdot 2\text{H}_2\text{O}$ has been determined by Thorup and Soling.¹ Its space group is $Pcca$ with $Z=4$ and $a=8.914$ Å, $b=7.174$ Å, and $c=11.360$ Å. In the a direction -Co-Cl-Co-chains exist. The compound is isostructural with $\text{CsMnCl}_3 \cdot 2\text{H}_2\text{O}$.^{2,3}

Recently, Herweijer, de Jonge, Botterman, Bongaarts, and Cowen⁴ studied the magnetic properties of $\text{CsCoCl}_3 \cdot 2\text{H}_2\text{O}$ by means of specific-heat, NMR, magnetic susceptibility, magnetization, and antiferromagnetic-resonance (AFMR) measurements. From this investigation the following conclusions were drawn.

Probably the magnetic space group is $P_{2b}cca'$. In this space group no b components are allowed for the magnetic moments, but a and c components are allowed and present, the angle ϕ between the magnetic moments and the c axis being 10° . The four-sublattice system can be described as sheets of moments in the ac planes coupled almost antiferromagnetically along a and ferromagnetically along c . Due to the canting over 10° a net moment along a is found (Fig. 1). Moments in adjacent sheets are coupled antiferromagnetically.

The interaction is Ising-like with very strong exchange along the a axis and much weaker interactions in the b and c directions. A Néel point is found at 3.38–3.40 K, but from the fact that only 16% of the theoretical entropy appears under the specific-heat peak at this temperature it is concluded that above this temperature an ordering of lower dimensionality persists. Therefore, $\text{CsCoCl}_3 \cdot 2\text{H}_2\text{O}$ is considered as an example of an Ising-like linear-chain antiferromagnet.

In the work presented in this paper an attempt has been made to obtain further support, by means of neutron scattering, for the above-mentioned conclusions. The measurements and conclusions to be treated in the following paragraphs are confirmation of the magnetic space group, a determination of the angle between the magnetic moment and the c axis, a study of the short-range-order spin correlations in the a and b directions in the vicinity of and above the Néel point, and a measurement of the temperature dependence of the magnetization.

II. EXPERIMENTAL

Crystals of $\text{CsCoCl}_3 \cdot 2\text{H}_2\text{O}$ to be used in the single-crystal work were grown by slow evaporation at room temperature of an aqueous solution of CoCl_2 and CsCl in a molar ratio of 4.8 : 1. The deep-violet crystals were much less developed in the c direction than in the other directions. The crystal selected for the diffraction work has been

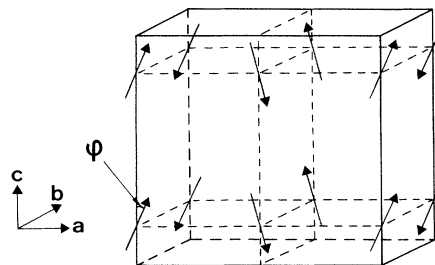


FIG. 1. Arrangement of the magnetic moments according to the magnetic space group $P_{2b}cca'$. All spins are in the ac plane.

shaped to a cylinder with a diameter of 6 mm and a thickness of 1 mm, the cylinder axis being roughly parallel to c .

Special care has to be taken when storing the crystals since, when exposed to the atmosphere at room temperature, the dihydrate converts into the blue anhydrate. The samples can be stored at temperatures below -5°C in a sealed container. For the powder work a deuterated sample has been prepared.

Neutron-scattering data were collected on a double-axis diffractometer at the high-flux reactor at Petten. In the powder work and the experiments described in Sec. IV, Soller slits with a horizontal divergence of $30'$ were placed before the monochromator [Cu-(111)] and in front of the BF_3 counter. The neutron wavelength was 2.57 \AA ; the second-order contamination was removed by means of a pyrolytic-graphite filter.⁵

Temperature control was achieved by regulating the pressure of the helium bath in which the sample was immersed. Pressure could be kept constant within 1 mm, corresponding to an uncertainty of about 0.003 K in the temperature region around T_N .

III. CRYSTALLOGRAPHIC AND MAGNETIC STRUCTURE

In order to check the crystallographic structure¹ and to determine the positions of the two hydrogen atoms, a powder diagram at 100 K has been collected. The final parameters resulting from a least-squares profile refinement⁶ are listed in Table I. For the hydrogen positions the parameters in $\text{CsMnCl}_3 \cdot 2\text{H}_2\text{O}$ as determined by nuclear-quadrupole resonance⁷ (NQR) were used as starting values.

In a powder diagram at 1.3 K a number of magnetic peaks appeared that could be indexed on the

basis of the magnetic unit cell mentioned above. The extra reflections fulfill the condition h odd, l even. This, combined with the fact that the position of the Co atom is $(0, 0.47, \frac{1}{4})$, satisfies the space group $P_{2_1}cca'$ with a small value for the angle ϕ , in accordance with the NMR result.⁴ The positional parameters and the values for the a and c components of the Co moment are listed in Table I. The angle ϕ following from this result is $17^\circ \pm 6^\circ$.

As the existence of a nonzero value for the a component of the Co moment is of great importance for the interpretation of the jump in the M - H curve and of the spin-cluster resonance data,⁴ magnitude and direction of this moment were also determined from a single-crystal sample.

Due to the shape of the crystal the collecting of intensities was limited to the $[hk0]$ planes. Further, it should be realized that since absorption and extinction effects may be large the systematic errors in this experiment can be very important. The observation of a nonzero $(0\frac{1}{2}0)$ intensity is conclusive for the existence of a magnetic a component and thus for the canted character of the spin structure.

The values for μ_x and μ_z that fit the observed single-crystal intensities are $0.9\mu_B$ and $2.4\mu_B$, respectively, which lead to $\mu_{\text{Co}} = 2.5\mu_B$ and $\phi = 21^\circ$. Because of the above-mentioned uncertainties in this experiment it is concluded that these values are not inconsistent with the powder results as given in Table I. The values quoted in Ref. 4 are $\mu_{\text{Co}} = (2.5 \pm 0.3)\mu_B$ and $\phi \approx 10^\circ$.

IV. MAGNETIZATION AND SHORT-RANGE SPIN ORDER

Scans were made through the reciprocal-lattice point $(1\frac{1}{2}0)$ in directions parallel to a^* ($h\frac{1}{2}0$) and to b^* ($1k0$) at temperatures between 1.2 and 4.2 K .

TABLE I. Magnetic and structural parameters in $\text{CsCoCl}_3 \cdot 2\text{D}_2\text{O}$ as obtained from neutron powder diffraction.^a

Temp. (K)	100			1,3		
	x	y	z	x	y	z
Cs	$\frac{1}{4}$	0	0.148(3)	$\frac{1}{4}$	0	0.150(4)
Co	0	0.469(5)	$\frac{1}{4}$	0	0.478(6)	$\frac{1}{4}$
Cl 1	$\frac{1}{4}$	$\frac{1}{2}$	0.149(2)	$\frac{1}{4}$	$\frac{1}{2}$	0.150(2)
Cl 2	0.088(1)	0.227(1)	0.389(1)	0.087(1)	0.231(1)	0.391(1)
O	0.066(2)	0.701(3)	0.365(2)	0.065(2)	0.728(3)	0.363(1)
D ₁	0.023(2)	0.685(3)	0.444(2)	0.027(2)	0.674(2)	0.444(2)
D ₂	0.166(2)	0.679(2)	0.378(2)	0.166(2)	0.676(2)	0.383(2)
a (\AA)	8.889(1)			8.887(1)		
b (\AA)	7.118(1)			7.104(1)		
c (\AA)	11.313(1)			11.312(2)		
μ_x				0.7(2) μ_B		
μ_z				2.4(2) μ_B		
μ (Co)				2.5(2) μ_B		
ϕ				17(6) $^\circ$		

^aStandard deviations, based on statistics only, in units of the last decimal place are given in parentheses.

The observed scattering profiles at temperatures below 3.30 K were fitted by a Gaussian adjusting a scale factor S_B and a full width at half-maximum Γ_α ($\alpha = h, k$). The half-widths were essentially constant for each scan direction and were $0.015\alpha^*$ and $0.009b^*$.

At temperatures above 3.40 K, no Gaussian contribution was observable. The peaks were broadened, indicating the absence of long-range spin order in the sample.

The neutron cross section for scattering by a short-range-ordered spin system, in the quasistatic approximation,^{8,9}

$$\begin{aligned} \frac{d\sigma}{d\Omega} &\propto \sum_{j=-\infty}^{+\infty} \langle \hat{S}_i \cdot \hat{S}_{i+j} \rangle e^{i\vec{Q} \cdot (\vec{r}_i - \vec{r}_{i+j})} \\ &= -1 + 2 \sum_{j=0}^{+\infty} \langle \hat{S}_i \cdot \hat{S}_{i+j} \rangle \cos \vec{Q} \cdot (\vec{r}_i - \vec{r}_{i+j}). \end{aligned} \quad (1)$$

For scans through $(1\frac{1}{2}0)$ along a^* or b^* , one obtains

$$\frac{d\sigma}{d\Omega} \propto -1 + 2 \sum_{m=0}^{+\infty} \langle \hat{S}_{z,i} \cdot \hat{S}_{z,i+m} \rangle \cos(2\pi h_\alpha m/p), \quad (2)$$

where h_α is h or k , p is 2 or 1, respectively, and \hat{S}_z is a unit vector along the c component of the i th Co spin. For the correlation function the expression $\langle \hat{S}_{z,i} \cdot \hat{S}_{z,i+m} \rangle = U_\alpha^{|m|}$ is used. Then we have

$$\begin{aligned} \frac{d\sigma}{d\Omega} &\propto -1 + 2 \sum_{m=0}^{+\infty} U_\alpha^m \cos(2\pi h_\alpha m/p) \\ &= (1 - U_\alpha^2) / [1 + U_\alpha^2 - 2U_\alpha \cos(2\pi h_\alpha/p)]. \end{aligned} \quad (3)$$

It is noted that $\langle \hat{S}_{z,i} \cdot \hat{S}_{z,i+1} \rangle = U_\alpha = 2q_\alpha - 1$, where

q_α is the probability that two adjacent spins in the α direction are aligned incorrectly. In both the a and b directions, $-1 \leq U_\alpha \leq 0$. Thus, the intensity reaches a maximum for $h = 2n + 1$ for h scans and for $k = \frac{1}{2}(2n + 1)$ for k scans. This maximum intensity is given by

$$\left(\frac{d\sigma}{d\Omega} \right)_{\max} \propto \frac{1 - U_\alpha}{1 + U_\alpha}. \quad (4)$$

The minimum value, which shows up as a contribution to the background, is

$$\left(\frac{d\sigma}{d\Omega} \right)_{\min} \propto \frac{1 + U_\alpha}{1 - U_\alpha}. \quad (5)$$

In the vicinity of the maxima expression (3) reduces to a Lorentzian. The observed scattering profile is obtained by convoluting (3) with a Gaussian with half-width Γ_α , which represents the experimental resolution:

$$I(h_\alpha) \propto -1 + 2 \sum_{m=0}^{+\infty} U_\alpha^m e^{-m^2/4p^2\gamma} \cos(2\pi h_\alpha m/p), \quad (6)$$

where $\gamma = 4 \ln 2 / \Gamma_\alpha^2$. The correlation length κ_α^{-1} in units of atomic distances is

$$\kappa_\alpha^{-1} = (-\ln |U_\alpha|)^{-1}. \quad (7)$$

The observed profiles above 3.40 K were fitted to expression (6). In the fitting procedure, Γ_α was kept constant at the values found below 3.30 K and the parameters to be adjusted were the scale factor S_L and U_α .

At temperatures between 3.30 and 3.40 K the observed profile consisted of a Lorentzian-shaped

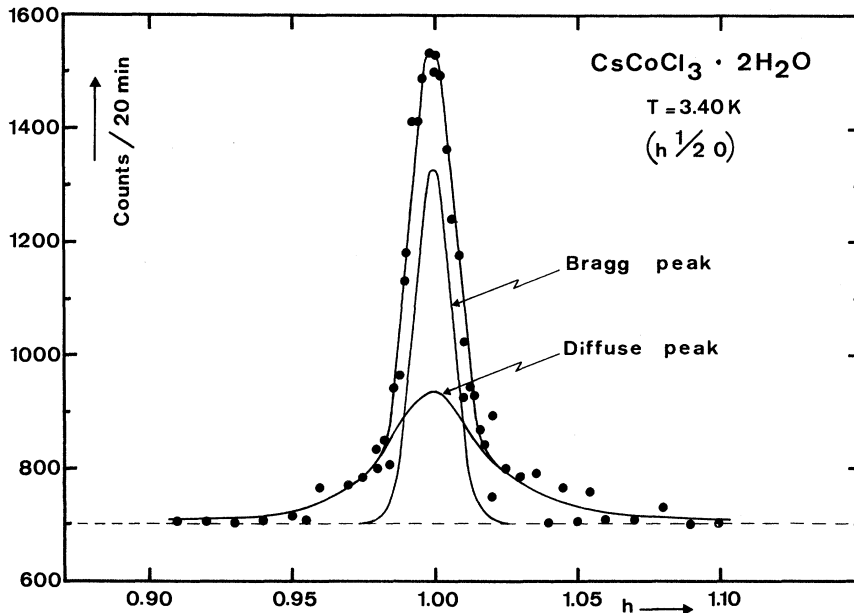


FIG. 2. Example of the co-existence of long- and short-range order near the Néel point. Drawn lines represent the best fit to the measurements as mentioned in the text.

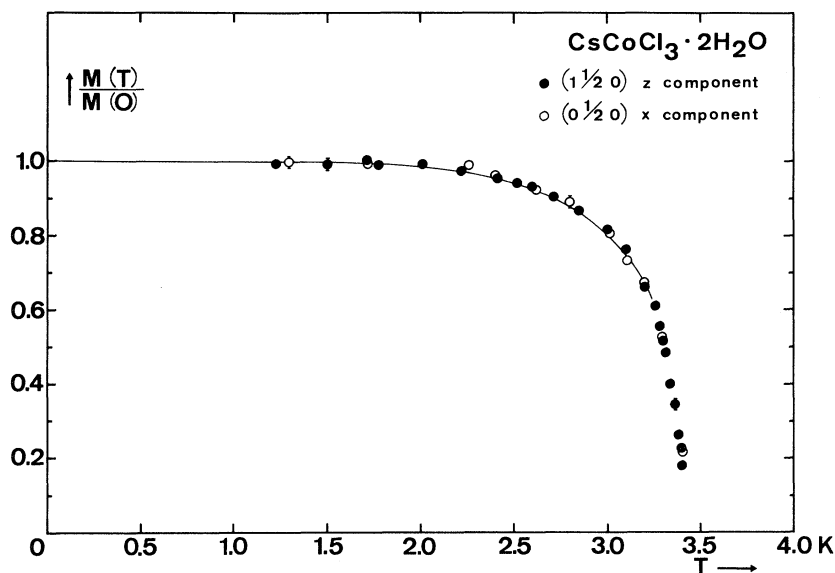


FIG. 3. Reduced sublattice magnetization as a function of temperature for the x and z component of the magnetic moment. The drawn line represents the NMR results of Ref. 3.

diffuse part with a Bragg peak superimposed on it. These two parts were separated by means of a fitting procedure with parameters S_B , S_L , and U_α . A typical example of such a profile is shown in Fig. 2.

The magnetization, determined as the square root of the Bragg intensity and reduced to 1 at $T=0$, is given in Fig. 3. To check whether the angle ϕ between moment and c axis changes in this temperature region the intensity of the Bragg peak at $(0\frac{1}{2}0)$ was also determined as a function of T . This intensity represents the a component of the Co moment. It is seen that within the experimental accuracy no moment rotation occurs. In Fig. 2 also the magnetization obtained with NMR⁴ is given. The agreement is satisfactory. The diffraction method, however, permits measurements closer to the Néel point.

The magnetization in the critical region is described by

$$\frac{M(T)}{M(0)} = A \left(1 - \frac{T}{T_N}\right)^\beta. \quad (8)$$

The data in the interval $3.20 \leq T \leq 3.39$ K were fitted by this equation. Including data obtained at lower temperatures resulted in a somewhat poorer fit. The final values and standard deviations are

$$A = 2.34 \pm 0.18,$$

$$T_N = (3.404 \pm 0.003) \text{ K},$$

$$\beta = 0.44 \pm 0.03.$$

This fit is presented in Fig. 4.

Some typical peak shapes of the diffuse scattering ($T > 3.40$ K) for both scan directions are shown in Figs. 5 and 6. In Fig. 7 the temperature de-

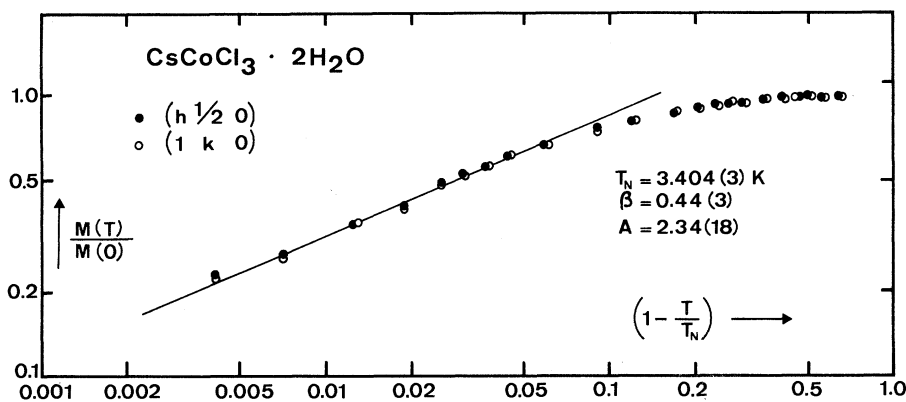


FIG. 4. Reduced sublattice magnetization as a function of temperature near the Néel point. The drawn line represents the best fit of the measurements for $3.20 \leq T \leq 3.39$ K to $M(T)/M(0) = A(1 - T/T_N)^\beta$.

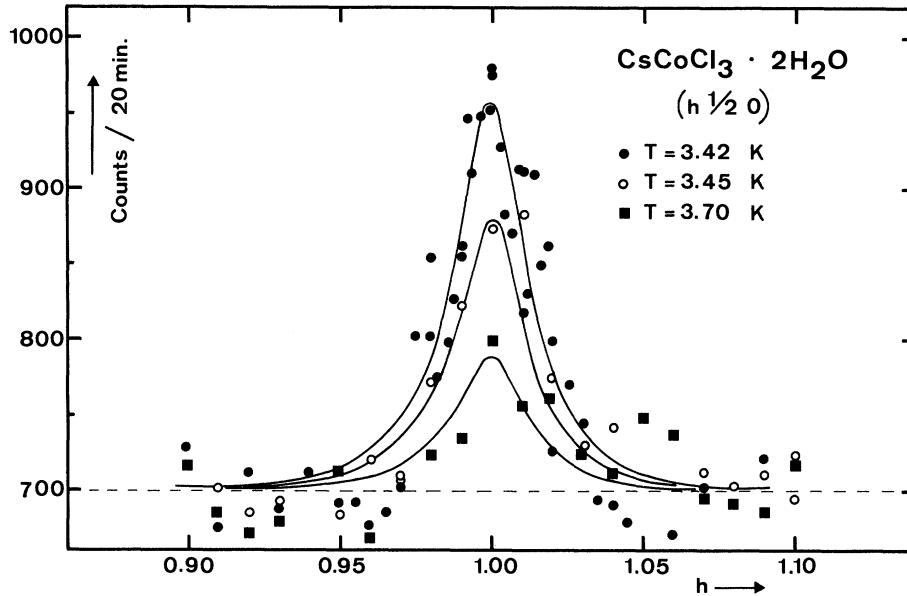


FIG. 5. Typical examples of observed scattering profile of scans ($h\frac{1}{2}0$) at different temperatures above the Néel point. Drawn lines represent the least-squares fits as mentioned in the text. Note that zero of the intensity scale is not shown.

pendence of U_a and U_b is given. It is seen that the intrachain correlation (in the chains parallel to a) varies slowly with temperature while the interchain correlation is strongly dependent on the temperature and reaches a maximum at T_N . The correlation length in the chains is about 89 \AA while the interchain correlation is 43 \AA at T_N and 12 \AA at 3.7 K .

The peak intensity from Eq. (4) is plotted in Fig. 8. As expected, this intensity diverges at T_N .

In order to calculate from the obtained U_a values an estimate for the intrachain exchange interaction we use the following Hamiltonian in effective spin- $\frac{1}{2}$ variables for the energy of a linear antifer-

romagnetic Ising-like chain:

$$H_a = -J_a \sum_i S_i^z S_{i+1}^z .$$

This Hamiltonian is the same as used by Herweijer *et al.*⁴ Thus it becomes possible to compare our results with those obtained by these authors.

For such a system the correlation parameter U_a is related to J_a as¹⁰

$$U_a = \tanh K \text{ with } K = J_a S^2 / kT .$$

From Fig. 7, it is seen that from the present data the value of J_a can be estimated as $25 < |J_a| < 35 \text{ K}$.

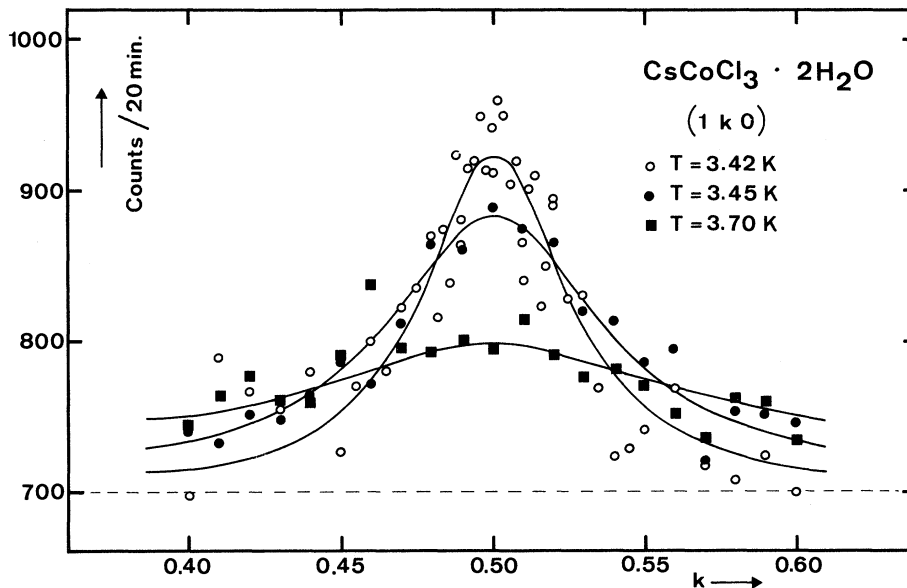


FIG. 6. Typical examples of observed scattering profile of scans ($1k0$) at different temperatures. Drawn lines represent the least-squares fits as mentioned in the text.

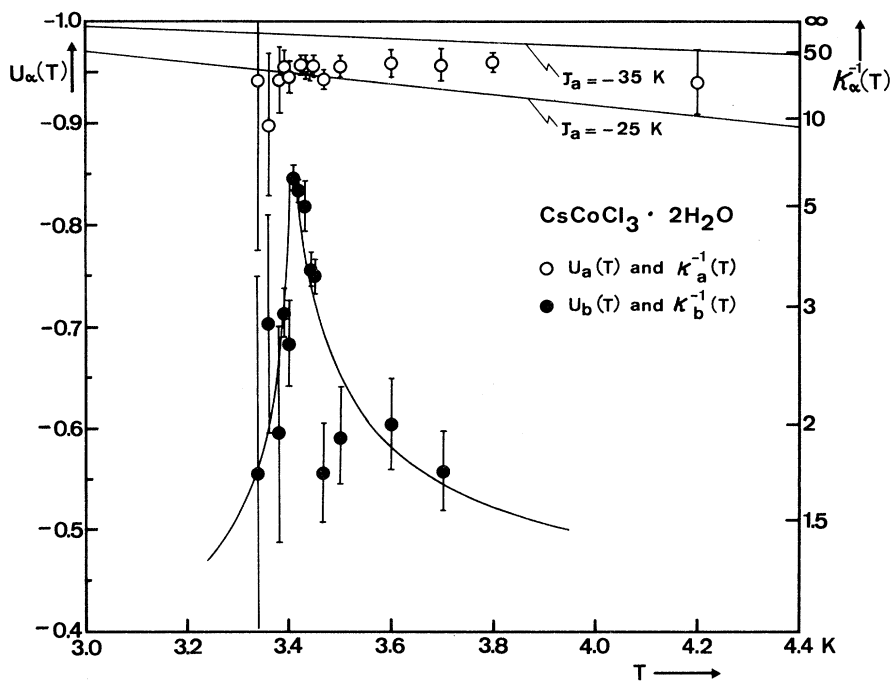


FIG. 7. Values of $U_\alpha(T)$ (left-hand scale) and the correlation length $\kappa_\alpha^{-1}(T)$ (right-hand scale) in units of interatomic distances along a and b as a function of temperature. The drawn lines for $U_a(T)$ represent the calculated curves for an Ising linear chain.

V. CONCLUSIONS AND DISCUSSIONS

$\text{CsCoCl}_3 \cdot 2\text{H}_2\text{O}$ was confirmed to possess the magnetic space group $P_{21}cca'$. The value for the Co moments, $(2.5 \pm 0.2)\mu_B$, agrees rather well with the values quoted in Ref. 4. The angle ϕ , between moment and c axis, $17^\circ \pm 6^\circ$, is not significantly higher than the value of 10° given in the same paper.

It should be noted that the value for μ_x which can

be deduced from the jump at H_c in the σ - H curve at $T = 1.1$ K in Ref. 4, $\mu_x = 0.6\mu_B$, agrees with our powder results.

The variation of the sublattice magnetization with temperature as determined in the present work agrees closely with that obtained by means of NMR.⁴ Also in agreement with NMR data¹¹ is the result that the angle ϕ does not change between 1.1 K and T_N .

The value for the Néel point obtained by a least-

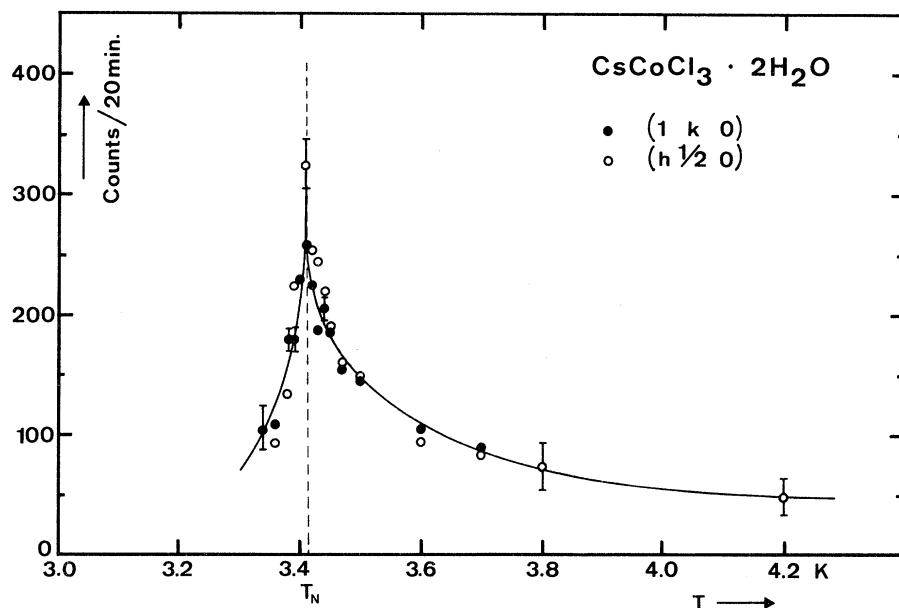


FIG. 8. Peak intensity of the Lorentz profiles from the $(h\frac{1}{2}0)$ and $(1k0)$ scans as a function of temperature. Note the diverging at the transition point.

squares fit to the power law in the critical region ($T_N = 3.40$ K) differs somewhat from the values resulting from specific-heat and NMR measurements ($T_N = 3.38$ K). It should be admitted, however, that the final value can be influenced by a suitable selection of the temperature region in which the fit is performed and the same is probably true for the specific-heat and NMR data.

The value for the critical index $\beta (= 0.44)$ can be compared with the value of $\frac{5}{16}$ predicted for a three-dimensional Ising-like system,¹² but it is very questionable whether this comparison is relevant.

There is a very striking difference in the behavior of the intrachain and the interchain correlations which reflects the linear character of the system. The correlation length in the chain remains practically constant (~ 20 atomic distances) up to 4.2 K.

The interchain correlation length shows a maximum at T_N . It decreases very sharply at decreasing temperatures and somewhat more slowly when the temperature increases. If one wishes to obtain a picture for the ordering-disordering process it should be realized that these correlation lengths represent the correlation in the short-range-ordered parts of the structure.

At $T=0$ there is only long-range order present in the system; each spin is aligned according to the ideal ordering scheme. When the temperature is increased chains of spins (along \vec{a}), which are located at different places in the lattice and isolated from each other, turn over (flip) their orientation. The average length (in atomic distances) of such a flipped row is $q_a^{-1} = 2/(1 + U_a)$. The number of

flipped rows increases with increasing temperature but they remain physically isolated from each other if the temperature is not too close to T_N . When the temperature approaches T_N there will be a tendency for the flipped rows to cluster. This then gives rise to an increase of the correlation length as the dimensions of the flipped regions increase.

At T_N the number of flipped and unflipped spins has become equal and at still higher temperature the clusters break up again and the interchain correlation goes down while the intrachain correlation remains practically constant.

For a description of the analogous process in a three-dimensional magnetic system the reader is referred to Stanley.¹³ It was not possible to obtain data at temperatures higher than 4.2 K since the intensity became very low because of the spreading out of the scattering power over planes in reciprocal space.

The value for the intrachain interaction $25 < |J_a| < 35$ K is considerably higher than the AFMR result: $|J_a| = 13$ K, but it should be realized that in

Smith and Friedberg¹⁵ use the following Hamiltonian for a linear $S = \frac{5}{2}$ Heisenberg chain:

$$H_a = -2J_a \sum_i \vec{S}_i \vec{S}_{i+1} .$$

The same Hamiltonian is used by Skalyo *et al.*² and they relate the correlation parameter U_a with the intrachain exchange interaction J_a as

$$U_a = \coth K - (1/K) \quad \text{with } K = 2J_a S(S+1)/kT .$$

In Fig. 9 the U_a values obtained as given above are

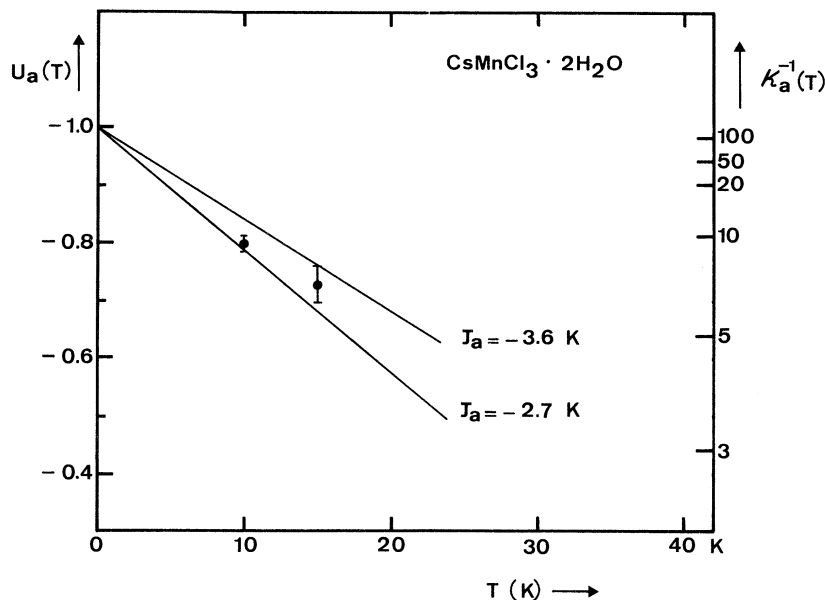


FIG. 9. Values of $U_a(T)$ (left-hand scale) and correlation length κ_a^{-1} (right-hand scale) in units of interatomic distances as a function of temperature in CsMnCl3 \cdot 2H2O as obtained from the experimental data of Skalyo *et al.* (Ref. 2). The drawn lines for $U_a(T)$ represent the calculated values for a linear Heisenberg chain.

represented together with theoretical lines for $U_a(T)$. This latter value has an uncertainty of a factor of 5.⁴ A serious objection against our present result is the neglecting of all non-Ising terms in the Hamiltonian.

The observation of the long intrachain correlation lengths can be considered as extra evidence for the Ising character of the interactions. In the case of a Heisenberg system the expression for U_a is

$$U_a = \coth K - (1/K),$$

which should lead to a value $J_a = -320$ K, a value which can be considered as very unlikely.

ACKNOWLEDGMENTS

The authors wish to thank Professor J. A. Cowen for the suggestion of the problem and kind advice, Professor P. van der Leeden and Dr. W. J. M. de Jonge for their continuing interest, Dr. B. O. Loopstra for his assistance in the initial stage of the experiment, and Dr. J. Skalyo, Jr. for a fruitful correspondence relating to his experimental work. The helpful assistance of J. F. Strang and P. H. J. Disseldorp with the experimental part of the work is very much appreciated.

APPENDIX

The correlation lengths in $\text{CsMnCl}_3 \cdot 2\text{H}_2\text{O}$ quoted by Skalyo *et al.*² from the scattering profiles are in error by a factor 2π for their *A* scans and a factor π for the *B* scans.¹⁴

The correct value for the interchain correlation at 5.5 K is ≈ 7 Å. In order to obtain the values for the intrachain correlation, we applied our least-squares-fitting method to the profiles given in Fig. 4 of Skalyo *et al.*² We obtained values of 20 Å at 10 K and 14 Å at 15 K. In the fitting procedure the value of $0.05a^*$ for Γ_h was used. It was not possible to obtain accurate correlation lengths at higher temperatures because the background levels are not known with sufficient accuracy.

From this figure it is seen that the experimental U_a values lead to $2.7 < |J_a| < 3.6$ K. This result is in good agreement with the value $J_a = -3.115$ K obtained by Smith and Friedberg¹⁵ by an analysis of the susceptibility and with the value $J_a = (3.57 \pm 0.02)$ K obtained by Skalyo *et al.*¹⁶ from magnon measurements.

It should be kept in mind when comparing the J_a of the Mn salt with the value obtained in Sec. V for the Co salt that the J_a 's given are related to different definitions of the Hamiltonian. Although this may be a bit confusing we preferred to keep the description for the two compounds consistent with the original papers, Refs. 2 and 4.

*Present address: Reactor Centrum Nederland, Petten (Nh), The Netherlands.

¹N. Thorup and H. Soling, *Acta Chem. Scand.* **23**, 2933 (1969).

²J. Skalyo, Jr., G. Shirane, S. A. Friedberg, and H. Kobayashi, *Phys. Rev. B* **2**, 1310 (1970).

³S. J. Jensen, P. Andersen, and S. E. Rasmussen, *Acta Chem. Scand.* **16**, 1890 (1962).

⁴A. Herweijer, W. J. M. de Jonge, A. C. Botterman, A. L. M. Bongaarts, and J. A. Cowen, *Phys. Rev. B* **5**, 4618 (1972).

⁵B. O. Loopstra, *Nucl. Instr. Methods* **44**, 181 (1966).

⁶H. M. Rietveld, *J. Appl. Cryst.* **2**, 65 (1969).

⁷W. J. M. de Jonge, J. P. A. M. Hijmans, and E. C. A. Gevers, *Physica* **52**, 129 (1971).

⁸W. Marshall and R. D. Lowde, *Rept. Progr. Phys.* **31**, 705 (1968).

⁹A. Guinier, *X-Ray Diffraction* (Freeman, San Francisco, 1963), English ed., Chap. 6.

¹⁰M. E. Fisher, *Am. J. Phys.* **32**, 343 (1964).

¹¹W. J. M. de Jonge (private communication).

¹²M. E. Fisher, *Rept. Progr. Phys.* **30**, 615 (1967).

¹³H. E. Stanley, *Introduction to Phase Transitions and Critical Phenomena* (Clarendon, Oxford, England, 1971), p. 6.

¹⁴J. Skalyo, Jr. (private communication).

¹⁵T. Smith and S. A. Friedberg, *Phys. Rev.* **176**, 660 (1968).

¹⁶J. Skalyo, Jr., G. Shirane, S. A. Friedberg, and H. Kobayashi, *Phys. Rev. B* **2**, 4632 (1970).